J. Fluid Mech. (1987), *vol.* 174, *pp.* 495–519
Printed in Great Britain

The influence of a peripheral layer of different viscosity on peristaltic pumping with Newtonian fluids

By JAMES G. BRASSEUR†, STANLEY CORRSIN
Department of Chemical Engineering, The Johns Hopkins University, Baltimore, MD 21218, USA

AND NAN Q. LU
Department of Mechanical Engineering, The Johns Hopkins University, Baltimore, MD 21218, USA

(Received 5 August 1985 and in revised form 9 June 1986)

The analysis by Shapiro *et al.* (1969) of a two-dimensional peristaltic pump at small Reynolds number and with long wavelengths is extended to include a Newtonian peripheral layer adjacent to the wall to simulate the effect of a coating in physiological flows. An earlier analysis by Shukla *et al.* (1980) violates mass conservation because of an incorrect deduction of the interface shape. We present a detailed analysis of the effect of the peripheral layer on the fluid motions, the pumping characteristics, and the phenomena of reflux and trapping. For prescribed wall motion, a peripheral layer more viscous than the inner fluid improves pumping performance, while a less-viscous outer layer degrades performance. Even a very thin peripheral layer may substantially reduce pumping if the viscosity in this layer is very low relative to the inner region. The effects of the peripheral layer on reflux and trapping depend on the conditions which are held fixed while making the comparison. However, the general trend with decreasing peripheral-layer viscosity is towards an overall decrease in trapping, a decrease in reflux with fixed total volume flow rate, but an increase in reflux with fixed pressure head.

1. Introduction

A peristaltic pump is a device for pumping fluids, generally from a region of lower to higher pressure, by means of a contraction wave travelling along a tube-like structure. This travelling-wave phenomenon is referred to as 'peristaltis'. Peristalsis originated naturally as a means of pumping physiological fluids from one place in the body to another, and is the primary pumping mechanism in swallowing (and indeed all the way through the alimentary canal), in the ureter, the bile ducts, the ductus efferentes of the male reproductive tract, and even in some small blood vessels. Humankind has borrowed the idea and used it in applications where the material being pumped must not be contaminated (e.g. blood), or is corrosive and should not be in contact with the moving parts of ordinary pumping machinery.

Considerable analysis of the pumping characteristics and the physical mechanisms involved has been carried out, primarily for the case of a homogeneous Newtonian

† Current address: Department of Mechanical Engineering, Clemson University, Clemson, SC 29634-0921, USA.

fluid pumped by a periodic train of sinusoidal contractions. For the physiologically relevant limit of inertia-free flow with infinitely long waves, the classical analysis was given by Shapiro, Jaffrin & Weinberg (1969). The main features of this peristaltic pumping were described and the phenomena of reflux and trapping elucidated.† The next-order terms in the expansions to higher Reynolds numbers and wavenumbers were later calculated by Jaffrin (1973), and by Buthaud (1971), who found that the zeroth-order solution is good to small finite values of Reynolds number and wavenumber. This suggests that the approximations of no inertia and small curvature (which are relatively simple) are adequate for studying the primary mechanisms involved at small finite Reynolds and wave numbers. The analysis shows that, physically, pumping by peristalsis is effected primarily by frictional forces. Indeed, for any wave shape, fluid will be pumped when the tube is sufficiently occluded by the travelling waves (see Lykoudis & Roos 1970); with complete occlusion, a peristaltic pump is obviously a positive displacement pump. A summary of the analyses of Shapiro, Jaffrin and others is given by Jaffrin & Shapiro (1971).

There are of course differences between peristalsis as found in nature and the analyses described above. Physiologically, for example, the wall of the structure doing the pumping (the oesophagus, the ureter, etc.) is typically coated with a fluid with properties different from those of the fluid being pumped. Often one or both fluids are non-Newtonian. However, as a first step towards understanding the effect of a fluid coating on the transport, it is of interest to extend the single-fluid Newtonian analysis to include a Newtonian peripheral layer of different viscosity. Such an analysis was attempted by Shukla *et al.* (1980), limited to the case with a decrease in pressure in the flow direction. However, their analysis violates the condition that mass must be independently conserved in the peripheral layer and the inner layer. The error enters in their deduction of an interface shape, independent of viscosity ratio, that is not a streamline in the steady 'wave frame', as it should be. The error is repeated in a later publication (Shukla & Gupta 1982).

The goal of this paper is to solve the problem of a peristaltic pump with a Newtonian 'core' fluid and peripheral layer, analysing the effects of the peripheral layer on the pumping characteristics and the fluid motions, especially on reflux and trapping. We make the same approximations as Shapiro *et al.* (1969); inertial forces and curvature effects are neglected. Consistent with the usual definition of a pump, attention is focused on cases with a net increase in pressure in the flow direction, although the solution is applicable to any pressure gradient.

The details of the mathematical development for any general wave shape are given in the next section. In §3 the analysis for a sinusoidal wavetrain is presented, and in the final section the results are summarized and general conclusions drawn. For simplicity, this work is limited to the plane case. The principal differences between the two-dimensional and axisymmetric flows in the single-fluid problem appear in the parametric range in which reflux and trapping occur on a plot of relative volume flow rate versus relative occlusion (§3.7, figure 15). Furthermore, we consider here only the case where a peripheral layer exists adjacent to the wall of the peristaltic pump. When trapping occurs, it is also possible for the interface between the two fluids to fall within the trapped region, thus representing a bolus of one viscosity trapped within a fluid of another viscosity being carried along with the peristaltic wave. The analysis of bolus transport is currently under investigation.

† Reflux here refers to the condition whereby some fluid particles move, on the average, in a direction opposite to that in which there is net pumping. Trapping occurs when the tube is sufficiently occluded or the average flow rate sufficiently high that a bubble of 'trapped' fluid moves with the peristaltic wave at the wave speed.

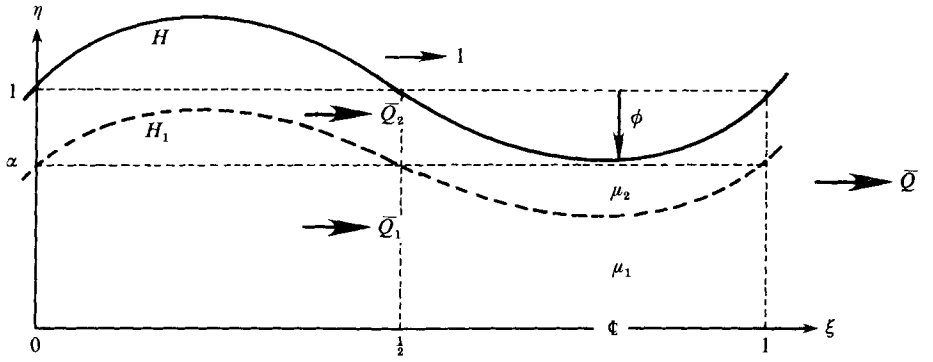

FIGURE 1. Non-dimensionalized peristaltic pump in the 'laboratory' frame at time $\tau = 0$. H and H_1 are the wall and interface shapes, periodic in $\xi - \tau$. $\alpha \equiv H_1(0)$. The wave moves to the right with non-dimensional speed 1.

2. The mathematical treatment

2.1. *The problem in the laboratory frame*

Consider a two-dimensional peristaltic pump, non-dimensionalized as shown in figure 1. Two infinite periodic wavetrains given by $H(\xi - \tau)$ travel symmetrically to the right down the walls of the channel. Transverse distances are non-dimensionalized with the average channel half-width a, axial distances with the wavelength λ, axial velocities with the wave speed c (so the non-dimensional wave speed is unity), and time (τ) with the wave period λ/c. Within the pump there is an inner core fluid with viscosity μ_1, and a peripheral layer with viscosity μ_2, both Newtonian, and separated by the interface $H_1(\xi - \tau)$, also periodic, but at this stage unknown.

For simplicity, the wave is sketched as a single Fourier mode; however, that constraint is not used in the general analysis. Each material point on the wall executes a periodic transverse motion in time. This requires slight periodic extension of the wall material (e.g. Taylor 1951), but in the small-slope approximation this is negligible.

For any periodic geometry, the total volume flow rate of the pump averaged over one cycle, denoted by $\bar{Q}$, will be time-independent. In addition to parameters describing the wall motion and peripheral layer, $\bar{Q}$ is a function of the mean pressure difference between the ends of the pump or, for an infinite wavetrain, the pressure difference ΔP across a unit wavelength.† The total average volume flow rate is given by the sum of the flow rates in the core fluid $\bar{Q}_1$, and in the peripheral fluid layer $\bar{Q}_2$:

$$\bar{Q} = \bar{Q}(\Delta P) = \bar{Q}_1 + \bar{Q}_2, \tag{2.1}$$

where $\bar{Q}_1$ is the integral of the axial velocity component up to H_1 and $\bar{Q}_2$ the integral from H_1 to H, each averaged over one period and non-dimensionalized by ca.

The dependent variables are non-dimensionalized as follows:

$$U = \frac{\hat{U}}{c} = \Psi_\eta, \quad V = \frac{\hat{V}}{kc} = -\Psi_\xi, \quad p = \hat{p}\frac{a^2}{\mu_1 \lambda c}, \tag{2.2}$$

where dimensional quantities are indicated with $\hat{}$, and $k = a/\lambda$ is a wavenumber. U and V are the ξ- and η-components of velocity respectively, and p is the pressure.

† Jaffrin & Shapiro (1971) show that for a single-fluid pump a periodic and infinite wavetrain is mathematically equivalent to a finite-length pump with an integral number of waves and constant pressure difference between the ends. This result can be extended to the peripheral layer case.

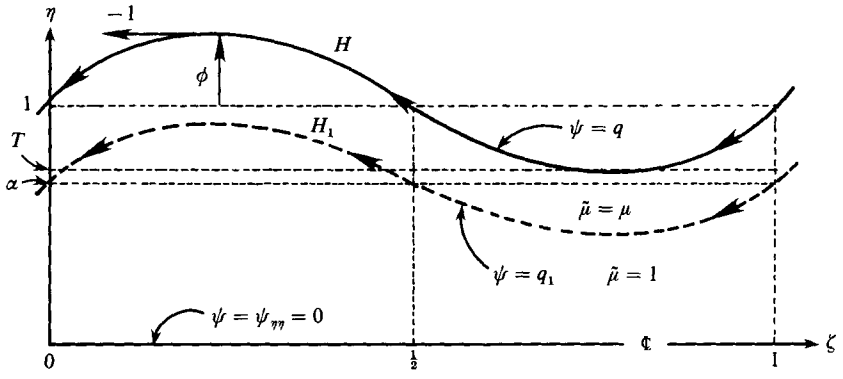

FIGURE 2. The peristaltic pump in the steady 'wave' frame. Material wall points move to the left with axial velocity -1, and fluid motions are periodic in $\zeta(\equiv \xi-\tau)$. Viscosity is non-dimensionalized with μ_1. T = average thickness of core fluid ($T \neq \alpha$ in general).

Since our interest is in the effect of variations in peripheral-layer viscosity, pressure is non-dimensionalized with the core-fluid viscosity, to be regarded as finite. The stream function Ψ, like the volume flow rates, is non-dimensionalized by ca.

In the limit of infinite wavelength and zero Reynolds number (defined by $Re = (ac\rho/\mu_1)\,k$), the Navier–Stokes equations reduce to

$$\left.\begin{aligned} \frac{\partial p}{\partial \xi} &= \frac{\partial}{\partial \eta}\left[\tilde{\mu}\frac{\partial U}{\partial \eta}\right], \\ \frac{\partial p}{\partial \eta} &= 0, \end{aligned}\right\} \tag{2.3}$$

where $\tilde{\mu}$ is the viscosity at the point (ξ, η) non-dimensionalized by μ_1. Neglecting inertia removes effects due to density and acceleration, and the approximation of infinite wavelength removes curvature effects. The result is a local rectilinear channel flow at every ξ, decoupled from every other ξ-location. Variations in ξ enter through the boundary conditions alone. At the interface between the core fluid and the peripheral layer there is a discontinuous jump in $\tilde{\mu}$. Since the shear stress $\tilde{\mu}U_\eta$ is continuous there, a discontinuity in vorticity $-U_\eta$ results.

2.2. *Solution in the wave frame*

In the 'laboratory' frame where the peristaltic wave is moving past the observer with the speed c, the flow field is unsteady. The steady frame of reference of figure 2 is obtained by moving with the wave so that the boundary shape remains constant in time. All variables are now periodic in $\zeta = \xi-\tau$. Transformations between frames are as follows, where wave-frame quantities are on the left and laboratory-frame quantities are on the right:

$$\left.\begin{aligned} \zeta = \xi-\tau, \quad \eta &= \eta, \\ u = U-1, \quad v &= V, \quad p = p, \\ \psi = \Psi-\eta, \quad q = \bar{Q}-1 &= q_1+q_2, \quad q_1 = \bar{Q}_1-T, \end{aligned}\right\} \tag{2.4}$$

where $T = \int_0^1 H_1(\zeta)\,\mathrm{d}\zeta$ is the average thickness of the inner layer.

We solve the problem in the wave frame in terms of the stream function ψ, which from (2.3) satisfies

$$\frac{\partial^2}{\partial\eta^2}\left[\tilde{\mu}\frac{\partial^2\psi}{\partial\eta^2}\right]=0, \tag{2.5a}$$

where

$$\tilde{\mu}=1, \quad 0\leqslant\eta<H_1, \tag{2.5b}$$

$$\tilde{\mu}=\frac{\mu_2}{\mu_1}\equiv\mu, \quad H_1<\eta\leqslant H, \tag{2.5c}$$

together with the conditions:

$$\psi=0, \quad \psi_{\eta\eta}=0, \quad \text{at } \eta=0, \tag{2.6a}$$

$$\psi_\eta=-1, \quad \psi=q=\text{const}, \quad \text{at } \eta=H, \tag{2.6b}$$

$$\psi=q_1=\text{const}, \quad \text{at } \eta=H_1. \tag{2.6c}$$

On the symmetry plane the stream function and the slope of the velocity profile are zero. The first condition at H is no-slip, the requirement that in the laboratory frame each material particle on the wall move only vertically. The other two are continuity conditions. Since mass must be conserved in the pump as a whole and independently in both the inner region and the peripheral layer, the outer boundary H and the interface H_1 must be streamlines in the steady frame.

Boundary conditions are also required across the 'ends' of the pump. This may be given by specifying either ΔP, or $\overline{Q}$, since ΔP and $\overline{Q}$ are interdependent. In the wave frame it is most convenient to specify $q(=\overline{Q}-1)$, and ΔP calculated by integrating the axial pressure gradient over one wavelength.

Integration of the equations of motion

A straightforward integration of (2.5a) with the boundary conditions (2.6a,b) yields the following, valid for any prescribed viscosity distribution $\tilde{\mu}(\eta;\zeta)$:

$$\psi(\eta;\zeta)=-\eta+(q+H)\frac{\int_0^\eta F(\eta)\,\mathrm{d}\eta}{\int_0^H F(\eta)\,\mathrm{d}\eta}, \tag{2.7a}$$

where

$$F(\eta)=\int_\eta^H\frac{s}{\tilde{\mu}}\,\mathrm{d}s. \tag{2.7b}$$

Once the viscosity variation is prescribed, (2.7) may be integrated to obtain the stream function and velocity fields. For the special case of two fluid layers, each of constant viscosity as defined by (2.5b,c), this yields

$$\psi=-\eta\left\{1-\tfrac{1}{2}(q+H)\left[\frac{\mu(3H_1^2-\eta^2)+3(H^2-H_1^2)}{H^3+(\mu-1)H_1^3}\right]\right\} \quad 0\leqslant\eta\leqslant H_1, \tag{2.8a}$$

$$\psi=-\eta+(q+H)\left[\frac{(\mu-1)H_1^3+\frac{1}{2}\eta(3H^2-\eta^2)}{H^3+(\mu-1)H_1^3}\right] \qquad H_1\leqslant\eta\leqslant H, \tag{2.8b}$$

with the corresponding velocity profile given by $\partial\psi/\partial\eta$. The axial pressure gradient is inferred from (2.3):

$$\frac{\mathrm{d}p}{\mathrm{d}\zeta}=-\frac{3\mu(q+H)}{H^3+(\mu-1)H_1^3}. \tag{2.9}$$

These results are for any wave shape $H(\zeta)$. We restrict this analysis to a simple sinusoidal wave given by

$$H(\zeta) = 1 + \phi \sin 2\pi\zeta. \tag{2.10}$$

The stream function, velocity field and pressure field may then be computed from (2.8) and (2.9) once the interface shape H_1 has been obtained.

The solution for the interface

A fourth-order algebraic for H_1 may be deduced from (2.8) by applying the continuity condition $\psi(H_1) = q_1$, Where q_1 is a constant:

$$[2(\mu-1)]H_1^4 + [2(\mu-1)q_1 - (q+H)(2\mu-3)]H_1^3 - [H^2(H+3q)]H_1 + [2q_1 H^3] = 0. \tag{2.11}$$

The coefficients of (2.11) are functions of the parameters μ, q and q_1; and of the wall height $H(\zeta)$. A consequence of the small-slope approximation, the ζ-dependence of H_1, enters locally through the ζ-dependence of H.

The value of q_1 in (2.11) is specified by a parameter describing the average thickness of the peripheral layer, most conveniently chosen as α, the value of H_1 at $\zeta = 0$ (also $\zeta = \frac{1}{2}, 1$). From (2.11) the relationship between α and q_1 is given by

$$q_1 = -\alpha\left\{1 - \tfrac{1}{2}\overline{Q}\left[\frac{3+\alpha^2(2\mu-3)}{1+(\mu-1)\alpha^3}\right]\right\}. \tag{2.12}$$

Having specified q_1 through α, (2.11) is solved by radicals (e.g. see Birkoff & MacLane 1953). The four roots are, in general, complex. Only one root is both real and in the range $0 \leqslant H_1 \leqslant H$. In the limit $\mu \to 1$, (2.11) reduces to a third-order algebraic equation describing a single streamline in a single-fluid pump.

The limit $\mu_2 \to \infty$

The condition that mass be conserved independently in the core fluid and peripheral layer, though properly stated, was not satisfied in the analyses of Shukla *et al.* (1980) and Shukla & Gupta (1982). There they deduce $H_1/H = \alpha$, independent of the viscosity ratio $\mu \equiv \mu_2/\mu_1$. The following argument shows that this is incorrect.

Consider the limit μ_2 approaching infinity with μ_1 finite (so $\mu \to \infty$). The no-slip condition at the wall requires that in this limit the velocity U in the peripheral layer goes to zero in the laboratory frame [let $\mu \to \infty$ in (2.8*b*)]. In the wave frame the axial velocity is therefore uniform and equal to -1, so

$$q_2 = \int_{H_1}^{H} u \, \mathrm{d}\eta \to -(H - H_1) \quad \text{as } \mu \to \infty. \tag{2.13}$$

Thus, since q_2 must be constant to conserve mass, in the limit $\mu \to \infty$ the peripheral layer approaches constant thickness $(1-\alpha)$ and

$$H_1(\zeta) \to H(\zeta) - (1-\alpha) \quad \text{as } \mu \to \infty. \tag{2.14}$$

Since the coefficients in (2.11) depend on μ, H_1 is in general a function of μ, approaching (2.14) in the limit $\mu \to \infty$.

The result $H_1/H = \alpha$, on the other hand, has no μ-dependence, nor does it have the limit required by (2.14). In fact (2.13) yields $q_2 = (\alpha - 1)H(x)$, violating the

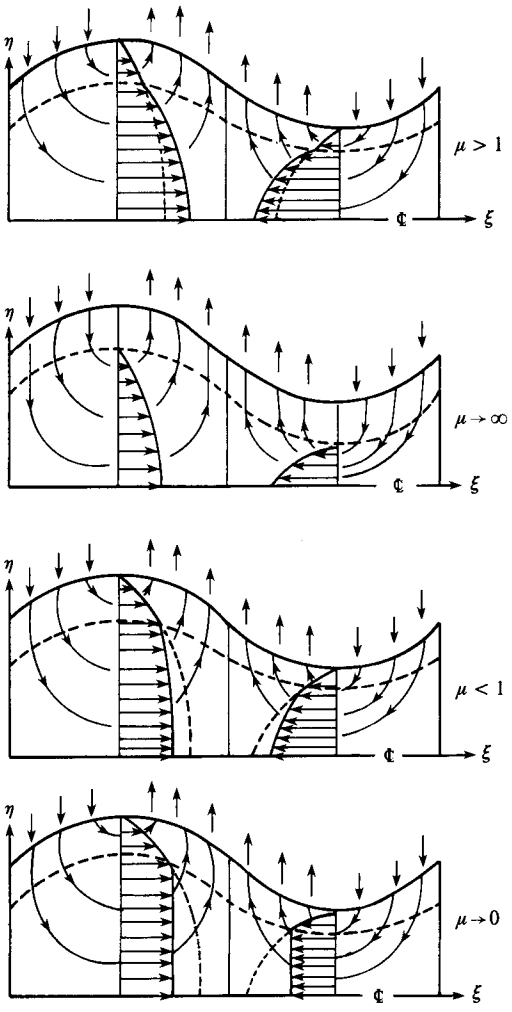

FIGURE 3. Qualitative instantaneous axial velocity profiles and streamlines at different $\mu \equiv \mu_2/\mu_1$. Dotted lines indicate parabolic extensions of the peripheral-layer profile.

continuity condition $q_2 =$ constant. It turns out that $H_1 \propto H$ violates continuity at all viscosity ratios (except in the limit $\alpha \to 1$, when $H_1 \to H$).

Note that in the limit $\mu \to \infty$ the peristaltic pump is again a single-fluid pump, but with greater occlusion. The peripheral layer becomes part of the solid boundary.†

3. The results

3.1. *The fluid motions*

Qualitative sketches of the instantaneous velocity and streamline fields in the laboratory frame are shown in figure 3. The discontinuity in slope at H_1 is required to maintain constant shear stress. As the viscosity ratio becomes infinite, the ξ

† A single-fluid pump could, of course, be defined from the outset with a wall of any shape and thickness. Here we consider a specified outer-wall shape and a peripheral fluid layer adjacent to the wall in the *limiting* process $\mu \to \infty$, whereby the peripheral layer becomes a constant-thickness solid layer.

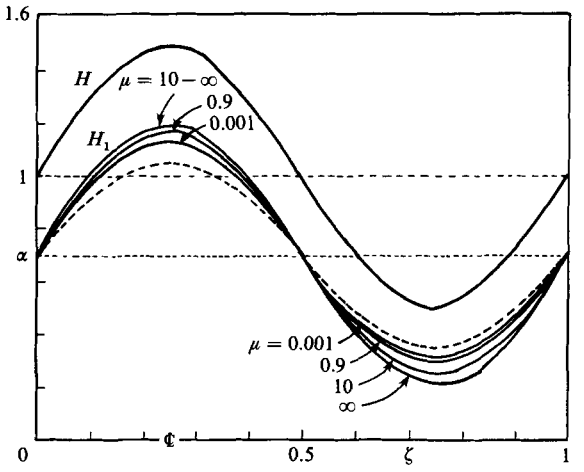

FIGURE 4. The variations in shape of the interface with viscosity ratio μ. $\phi = 0.5$, $\alpha = 0.7$, $\overline{Q} = 0.1$; ---, $H_1/H = \alpha$ (Shukla *et al.* 1980).

velocity component in the peripheral layer vanishes, producing a single phase pump with occlusion ϕ/α.

The limit $\mu \to 0$ is at first glance a curious one. The velocity in the inner region is constant in η, locally a plug flow. However, the U-velocity varies in ξ, so the inner region may not be interpreted as a rigid solid in this limit. The boundary condition at the wall requires that the inner region, like the peripheral layer, be deformable at all viscosity ratios since in the laboratory frame material points on the interface, together with the wall, move laterally. One must interpret the limit $\mu \to 0$ as one in which the peripheral-layer viscosity vanishes, as may be seen through examination of the dimensional forms of the equations for velocity and pressure gradient. This is a reflection of choosing μ_1 in non-dimensionalizing the equations of motion, whereby μ_1 must be regarded as finite as μ is varied. Thus, in the limit $\mu \to 0$, (2.9) yields $\mathrm{d}p/\mathrm{d}\zeta \to 0$ with the consequence that any finite pressure differential produces infinite flow rates in a peripheral layer of finite thickness (§§3.3, 3.8).

In the wave frame particle trajectories lie along streamlines. Depending on the occlusion ϕ and the volume flow rate $\overline{Q}$, two classes of patterns are possible for fixed μ as may be observed, for example, in figure 13. At large ϕ and $\overline{Q}$ (figure 13*b*, *c*) there is a region where the fluid is 'trapped' relative to the wave, moving with average velocity equal to the wave speed. Pumping also occurs in figure 13(*a*); although trapping does result in net pumping it is not a necessary condition for pumping to occur.

3.2. *The interface*

The interface is a streamline in the wave frame, as shown for example in figures 13 and 14. When no trapping exists there is no restriction on our choice for α. With trapping, however, we require that H_1 remain outside the trapped region, restricting α to values above a lower limit.

Figure 4 is an example showing the variation in shape of the interface with viscosity ratio. Low viscosity ratios are associated with thinner layers in the constricted region of the pump. As $\mu \to \infty$ the peripheral-layer thickness becomes uniform. The interface shape $H_1 \propto H$ of Shukla *et al.* (1980) is never obtained.

The thickness of the peripheral layer is most conveniently specified with the

parameter α. The difference between the average thickness of the inner core region T and α turns out to be at most about two per cent (note that $T \to \alpha$ as $\mu \to \infty$), so that $(1-\alpha)$ does in fact serve as an effective measure of the thickness of the peripheral layer.

3.3. *The pumping characteristics*

An integral of $\mathrm{d}p/\mathrm{d}\zeta$ (2.9) over one wavelength produces the relationship between the average volume flow rate $\overline{Q}$ and the pressure rise per wavelength ΔP:

$$\overline{Q} = \overline{Q}_0 \left[1 - \frac{\Delta P}{\Delta P_0}\right]. \tag{3.1}$$

As a 'pump' the device operates against a positive pressure head ΔP in the range $0 \leqslant \Delta P \leqslant \Delta P_0$, and with positive flow rate $\overline{Q}$ in the range $0 \leqslant \overline{Q} \leqslant \overline{Q}_0$.† The functions $\overline{Q}_0$ and ΔP_0 are the maximum values in this range, $\overline{Q}_0$ defined as the value of $\overline{Q}$ when $\Delta P = 0$, and ΔP_0 the value of ΔP when $\overline{Q}_0 = 0$. These are given by

$$\overline{Q}_0 = 1 - \frac{\int_0^1 \beta(\zeta) \dfrac{\mathrm{d}\zeta}{H^2}}{\int_0^1 \beta(\zeta) \dfrac{\mathrm{d}\zeta}{H^3}}, \tag{3.2a}$$

$$\Delta P_0 = 3\mu \left[\int_0^1 \beta(\zeta) \frac{\mathrm{d}\zeta}{H^3} - \int_0^1 \beta(\zeta) \frac{\mathrm{d}\zeta}{H^2}\right], \tag{3.2b}$$

where

$$\beta(\zeta) = \left[1 + (\mu - 1)\left(\frac{H_1}{H}\right)^3\right]^{-1}.$$

When $\mu = 1, \beta = 1$ and (3.2) integrate to the single-fluid result of Shapiro *et al.* (1969)

$$\overline{Q}_0 = \frac{3\phi^2}{2+\phi^2}, \tag{3.3a}$$

$$\Delta P_0 = \frac{9\phi^2}{2(1-\phi^2)^{\frac{5}{2}}}. \tag{3.3b}$$

The overall pumping characteristics of a two-fluid peristaltic pump are illustrated in figures 5, 6 and 7, for $\alpha = 0.8$. In figure 5 the relationship between ΔP and $\overline{Q}$ is plotted at different viscosity ratios when $\phi = 0.7$. In the single-fluid pump $\overline{Q}$ and ΔP are related linearly at each occlusion value ϕ. In the two-fluid pump, however, β is a function of $\overline{Q}$ through H_1, producing a nonlinear dependence of ΔP on $\overline{Q}$. Only in the limits $\mu \to 1$ (when $\beta = 1$), $\mu \to 0$ (when $\Delta P = 0$) and $\mu \to \infty$ (again a single-fluid pump) are ΔP and $\overline{Q}$ linearly related.

The peripheral layer is found to have a large effect on the overall pumping characteristics. For prescribed wall motion, a larger viscosity in the peripheral layer ($\mu > 1$) dramatically increases the pumped volume flow rate $\overline{Q}$ compared with the single-fluid pump ($\mu = 1$) for fixed ΔP; for prescribed $\overline{Q}$, the pump can work against a greater pressure head. These effects are reversed when the peripheral layer has

† It should be remarked that the case in which the peristaltic wave and mean pressure gradient tend to move the fluids in the same direction ($\Delta P < 0$) is included in this analysis. No example has been computed because the fluid mechanically interesting phenomena, such as 'trapping' with partial occlusion and local marginal 'reflux', occur primarily when the pressure head acts in the direction opposite to the net flow. Indeed, 'reflux' can only occur with a positive pressure head. Nevertheless, 'co-pumping' may be physiologically relevant, e.g. in the intestines.

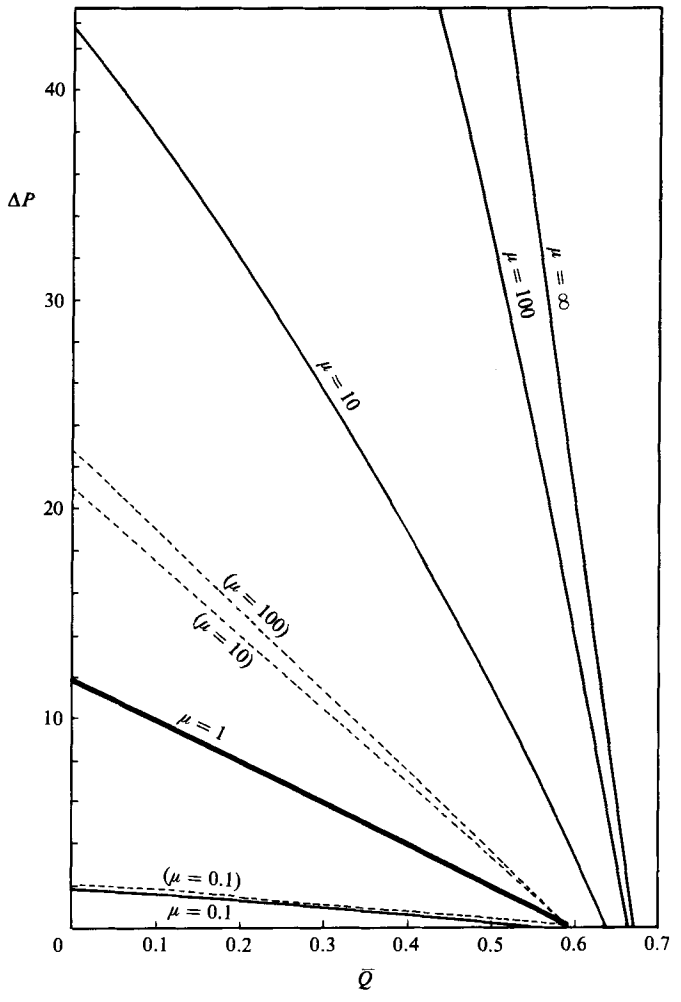

FIGURE 5. The pumping characteristics: $\overline{Q}$ versus ΔP for different μ. $\phi = 0.7$, $\alpha = 0.8$; ---, Shukla *et al.* (1980).

lower viscosity than the inner fluid ($\mu < 1$). In fact, as $\mu \to 0$, $\Delta P \to 0$ and the pump no longer pumps! This is not surprising, since peristaltic pumping depends on viscous forces which originate at the walls. When $\mu = 0$, any finite (positive) pressure differential ΔP produces infinite (negative) volume flow rates $\overline{Q}$. Infinite velocities occur in the peripheral layer where the viscosity is effectively zero (§3.8).

Figure 5 shows that Shukla *et al.* (1980) underestimate pumping performance at high viscosity ratios, and overestimate performance when $\mu < 1$. In contrast with (3.2), where both $\overline{Q}_0$ and ΔP_0 are functions of μ and $\overline{Q}$ is a nonlinear function of ΔP, constant H_1/H leads to a linear relationship between ΔP and $\overline{Q}$, no dependence of $\overline{Q}_0$ on μ, and incorrect ΔP_0.

Figures 6 and 7 show the dependence of $\overline{Q}_0$ and ΔP_0 on μ. Whereas $\overline{Q}_0$ is relatively insensitive to μ, ΔP_0 shows a much greater effect. As $\phi \to 0$, the peristaltic pump approaches a purely pressure-driven channel flow; consequently $\overline{Q}_0$ and $\Delta P_0 \to 0$. As $\phi \to 1$ all fluid becomes trapped and $\overline{Q}_0$ tends towards 1, the maximum flow rate attainable (the curves stop short of $\phi = 1$, however, since for α fixed a point is always

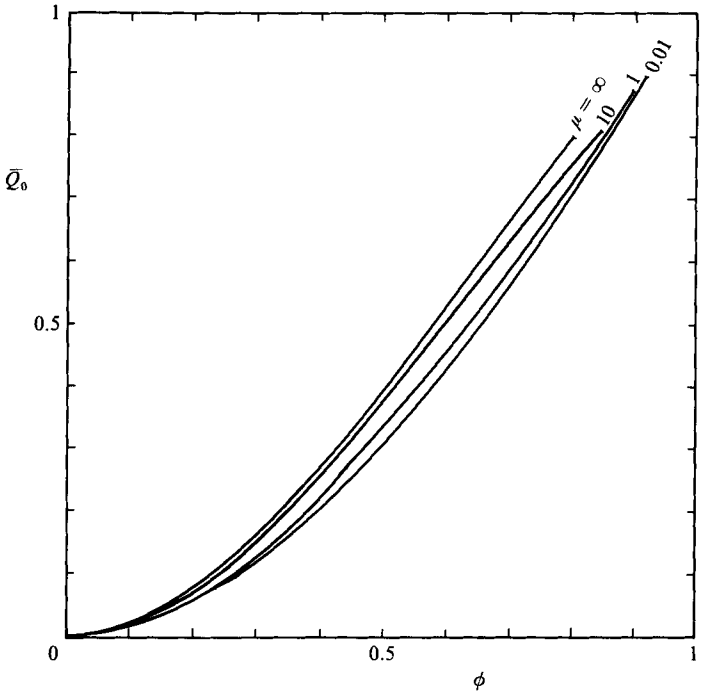

FIGURE 6. The variation of $\bar{Q}_0$ with ϕ for different μ. $\alpha = 0.8$.

reached where the interface moves into the trapped region; figure 15 has the same behaviour). In the limit $\phi \to 1$ an infinite pressure rise is required to force $\bar{Q}$ to zero. When $\phi < 1$, increasing the viscosity ratio increases ΔP_0,

The mechanical efficiency E of the two-fluid peristaltic pump compared with the single-fluid pump is shown in figure 8. Following Shapiro *et al.* (1969), efficiency is defined as the average rate (per wavelength) at which work is done by the moving fluid against a pressure head, divided by the average rate at which the walls do work on the fluid, where averages are taken over one period. The difference between E and unity is the rate at which energy is dissipated to internal energy relative to the power applied at the walls. For the two-fluid pump the efficiency is given by

$$E = \frac{\bar{Q}}{\phi} \frac{q \int_0^1 \beta(\zeta) \frac{\mathrm{d}\zeta}{H^3} + \int_0^1 \beta(\zeta) \frac{\mathrm{d}\zeta}{H^2}}{q \int_0^1 \beta(\zeta) \frac{\sin 2\pi\zeta}{H^3} \mathrm{d}\zeta + \int_0^1 \beta(\zeta) \frac{\sin 2\pi\zeta}{H^2} \mathrm{d}\zeta}, \tag{3.4}$$

where $q = \bar{Q} - 1$. Equation (3.4) integrates to the result given by Shapiro *et al.* when $\mu = 1$.

Figure 8 shows that greater occlusion increases efficiency at all viscosity ratios; a more-viscous peripheral layer improves efficiency, and a less-viscous layer degrades efficiency compared with a single-fluid pump. When $\phi = \alpha$, as in figure 8(*b*), the tube becomes totally occluded as $\mu \to \infty$, $\bar{Q}$ approaches $\bar{Q}_0$, and E is indeterminate. In the limit $\mu \to 0$, on the other hand, $\Delta P \to 0, \bar{Q} \to \bar{Q}_0$ (by definition), and the efficiency drops to zero. In this limit the pump can do no work.

The effect of the thickness of the peripheral layer is shown in figure 9 for $\mu = 0.1$

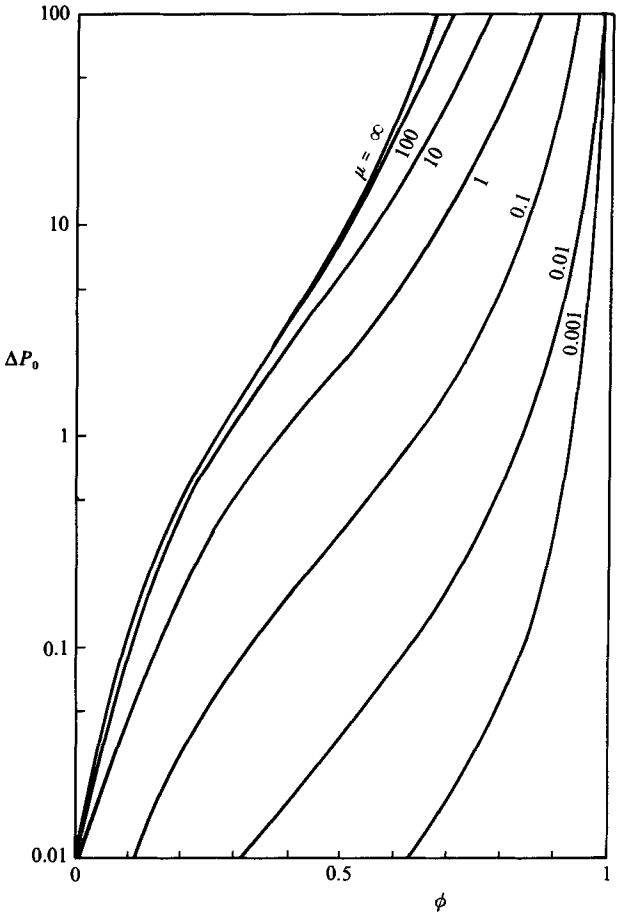

FIGURE 7. The variation of ΔP_0 with ϕ for different μ. $\alpha = 0.8$.

and 10. When $\mu > 1$, the peripheral layer apparently has a large effect only when the layer is rather thick. At small viscosity ratios, however, even a 1 % thick layer can easily reduce pumping by 50 % or more. Indeed, as $\mu \to 0$ peristalsis ceases to produce pumping with *any* finite-thickness peripheral layer.

Clearly pumping performance is strongly affected by the presence of a peripheral layer. In general, performance is enhanced when the peripheral layer is more viscous than the core fluid, and degraded when the peripheral layer is less viscous than the core fluid. The same conclusions may be drawn when one considers the effect of the peripheral layer on the core fluid alone (§3.8).

3.4. *The method of comparing two-fluid and single fluid pumps*

In the sections that follow we study the influence of the peripheral layer on reflux and trapping. In making the comparisons the wave shape and wave speed are held fixed (another possibility, for example, might be constant power input). We are at liberty, however, to choose either constant pressure head ΔP, or constant flow rate $\bar{Q}$ as end conditions. The distinction may be significant since a change in μ with constant $\bar{Q}$ is accompanied by a change in ΔP, whereas fixed ΔP is associated with a lower limit in μ below which $\bar{Q}$ becomes negative.

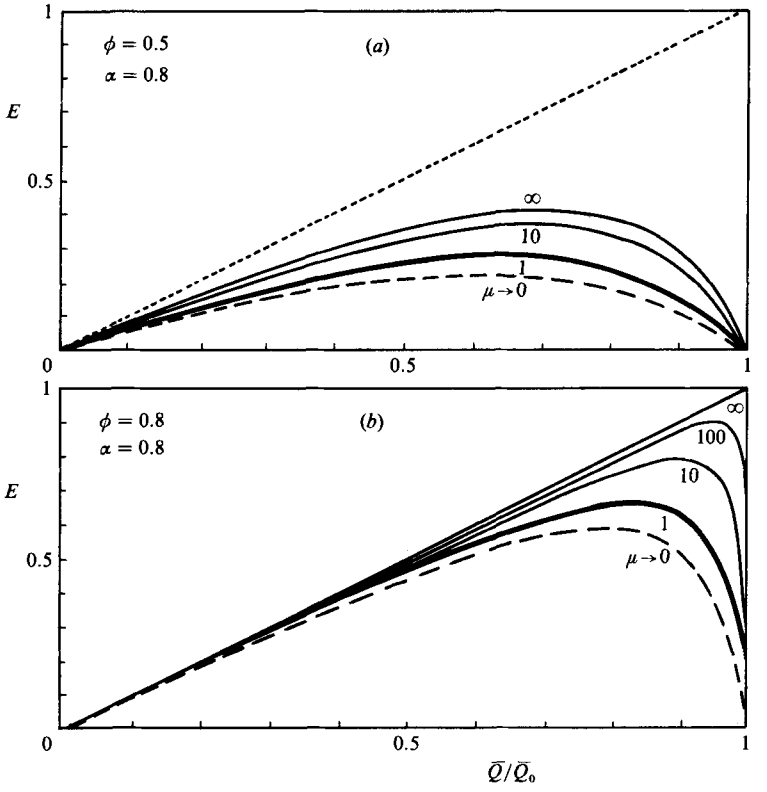

FIGURE 8. The mechanical efficiency of the two-fluid pump over the pumping range $0 \leqslant \bar{Q} \leqslant \bar{Q}_0$ for different μ. When $\phi = \alpha$, as $\mu \to \infty$ the tube becomes totally occluded (*b*).

Since fixed $\bar{Q}$ is more straightforward to compute and is not complicated by a lower limit in μ we consider the effect of the peripheral layer first with constant-volume flow rate. In §3.8 we discuss comparisons at constant pressure head – more suitable, perhaps, to the laboratory situation. It turns out that the effect of the peripheral layer does depend on how the comparisons are made.

3.5. *Reflux at constant* $\bar{Q}$

'Reflux' here refers to the presence of fluid particles that move, on the average, in a direction opposite to the net flow. The phenomenon has had physiological importance in that it implies the possible backward migration of bacteria against the direction in which physiological fluids are pumped. Our interest is to determine the effect of the peripheral layer on the regions in which reflux occurs, and on the amount of reflux in these regions.

As pointed out by Shapiro *et al.* (1969), the details of reflux depend on the trajectories of individual fluid particles and require use of material, or 'Lagrangian' coordinates. Consider the schematic in figure 10, where a particle trajectory is viewed in the laboratory frame as the peristaltic wave travels progressively to the right. The fluid particle moves through one 'particle period', the time it takes to return to the same position relative to the wave. The 'particle cycle' then repeats itself.† Super-

† Note that the particle period is not in general equal to the wave period (Shapiro *et al.* 1969).

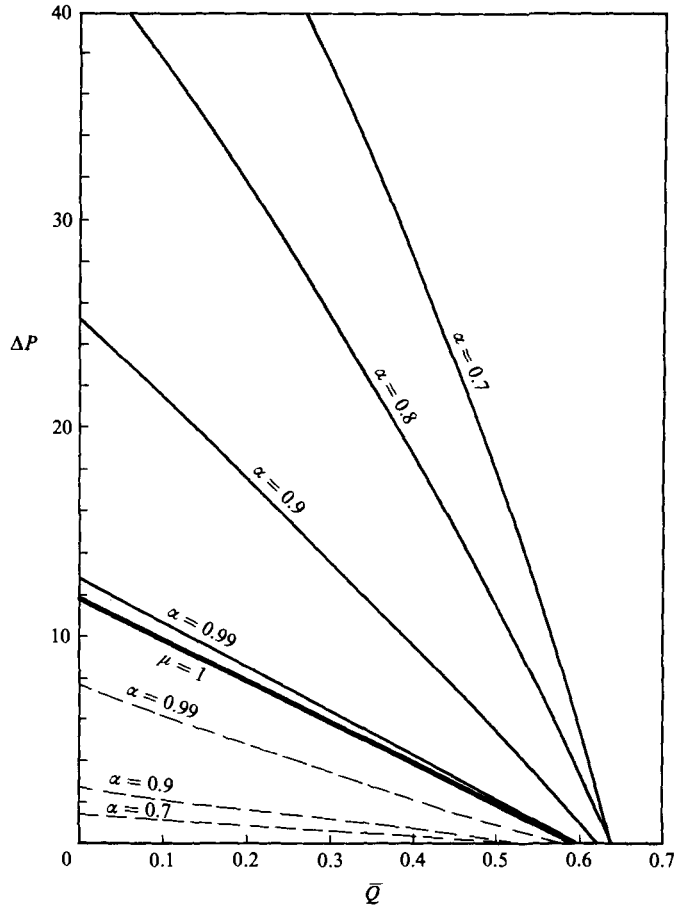

FIGURE 9. The effect of thickness of the peripheral layer: $\bar{Q}$ versus ΔP for different α when $\mu = 10, 0.1$. $\phi = 0.7$; —, $\mu = 10$; – – –, $\mu = 0.1$.

imposed on the laboratory frame are shown streamlines in the moving wave frame (boxed) which remain fixed relative to the moving wave. Since the particle moves along a streamline in the wave frame, it is always associated with the same wave-frame stream function ψ during its trajectory when viewed in the laboratory frame. It is evident from figure 10 that the average of any particle property over one particle cycle in the laboratory frame will yield the same value for all particles associated with the stream function ψ in the wave frame. After averaging, therefore, ψ may be used unambiguously as a marker of a fluid particle, i.e. as a material coordinate.

Following Shapiro *et al.* (1969), we average the axial volume flow rate between the centreline of the tube and the particle trajectory over one particle cycle in the laboratory frame. The volume flow $Q_\psi(\zeta)$ associated with a particle at the position ξ and time τ in the laboratory frame, and on the streamline ψ in the wave frame, is given by the transformation between Ψ and ψ in (2.4):

$$Q_\psi(\zeta) = \psi(\zeta) - \eta(\zeta; \psi), \tag{3.5}$$

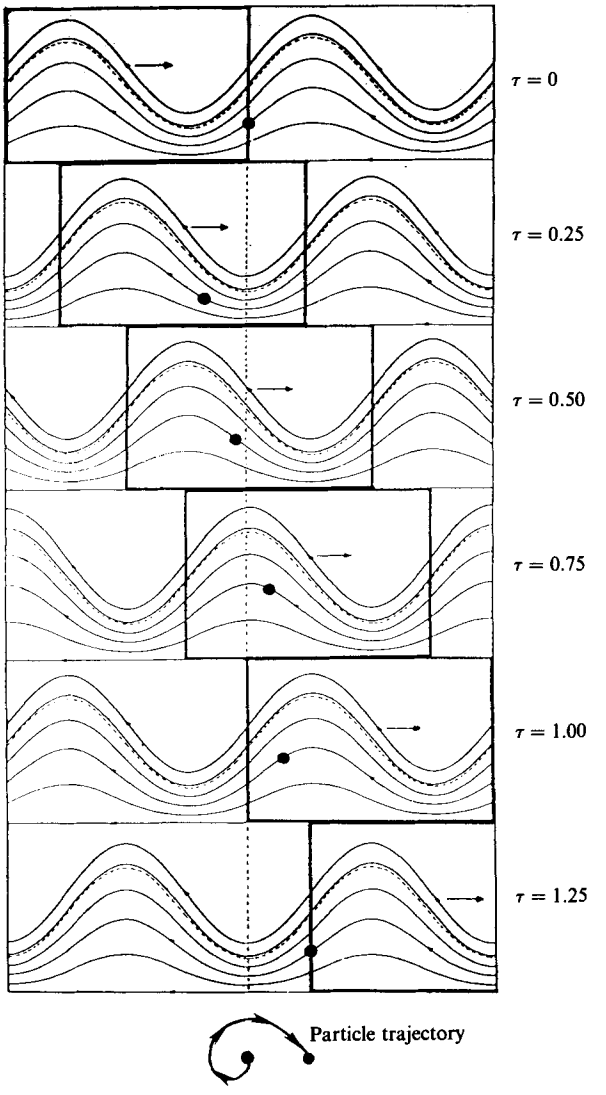

FIGURE 10. Example schematic of a particle trajectory in the laboratory frame. The peristaltic wave moves to the right; the streamlines in the wave frame (shown boxed) remain fixed relative to the moving wave. The particle trajectory in the laboratory frame is always associated with the same stream function ψ in the wave frame.

where $\eta(\zeta;\psi)$ is the position of the particle on the streamline ψ at a particular $\zeta(=\xi-\tau)$-location. Averaging over one particle cycle yields

$$\int_0^1 Q_\psi(\zeta)\,\mathrm{d}\zeta \equiv \overline{Q}_\psi = \psi - \int_0^1 \eta(\zeta;\psi)\,\mathrm{d}\zeta. \tag{3.6}$$

A plot of $\overline{Q}_\psi/\overline{Q}$ against ψ/q identifies the reflux zone. The wall is reached in the limit $\psi/q\to 1$, where $\overline{Q}_\psi/\overline{Q}\to 1$, and the centreline in the limit $\psi/q\to 0$ where $\overline{Q}_\psi/Q\to 0$. Reflux appears as a region where $\overline{Q}_\psi/\overline{Q}$ decreases with increasing ψ/q, so if a reflux

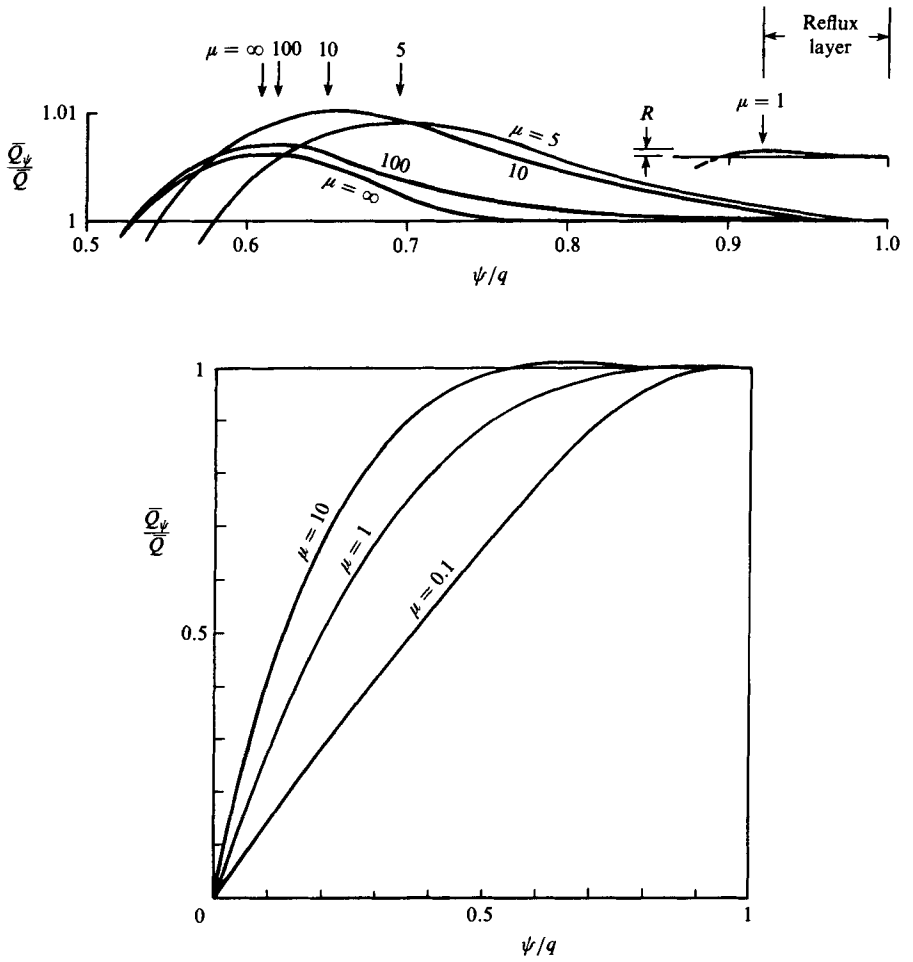

FIGURE 11. $\overline{Q}_\psi/\overline{Q}$ versus ψ/q with fixed $\overline{Q}$ for different μ. The reflux layer (the region with negative slope) spreads away from the wall with increasing μ. R = (volume flow rate in the reflux layer)/$\overline{Q}$. $\overline{Q} = 0.21$, $\phi = 0.5$, $\alpha = 0.8$.

layer exists along the wall, as was found by Shapiro *et al.* (1969) for the single-fluid case, $\overline{Q}_\psi/\overline{Q}$ should increase to a value greater than 1, then decrease to 1 at the wall.

A typical plot of $\overline{Q}_\psi/\overline{Q}$ against ψ/q is shown in figure 11 as a function of μ (holding $\overline{Q}$ fixed) for a case where reflux already exists when $\mu = 1$. The reflux zone is always adjacent to the wall; however, as the viscosity ratio increases, it spreads inward towards the centreline. At the same time, the flow in the peripheral layer decreases to zero at $\mu = \infty$, when the reflux layer has moved adjacent to the interface (which now becomes the new wall).

The reflux ratio R, defined as the volume flow rate in the reflux layer divided by the total volume flow rate $\overline{Q}$, is given by the peak value of $\overline{Q}_\psi/\overline{Q}$ above 1. A plot of R against μ is given in figure 12 for cases where reflux does and does not exist at $\mu = 1$. Reflux disappears for μ small, reaches a maximum as μ increases, and asymptotes to a non-zero value as $\mu \to \infty$.

The general conclusion that reflux increases with increasing viscosity ratio and may disappear at sufficiently small μ is valid when comparisons are made with volume flow rate held constant. We shall find the opposite trend when comparisons are made at constant pressure head.

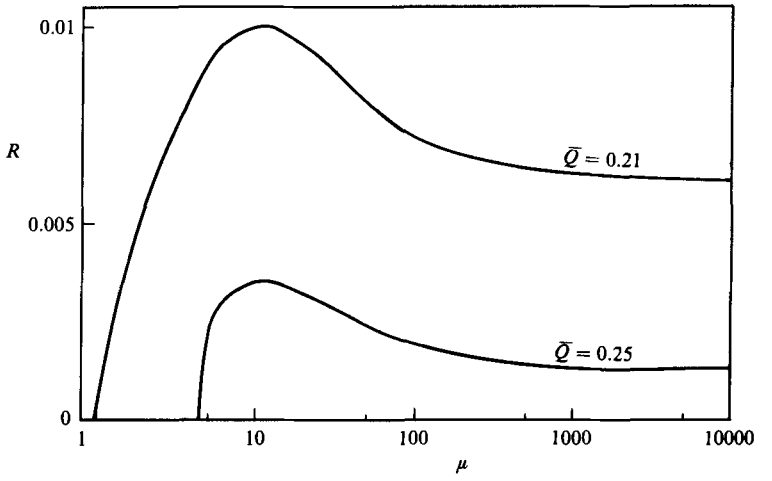

FIGURE 12. Variation in reflux ratio R with μ for fixed $\bar{Q}$. $\phi = 0.5$, $\alpha = 0.8$.

3.6. *Trapping at constant* $\bar{Q}$

Like the single-fluid pump, trapping occurs in the two-fluid pump at high flow rates and large occlusion as demonstrated in figure 13 for the case $\mu = 0.1$. The existence of a peripheral layer, however, has a strong influence on the size of the trapped region. Figure 14 shows that when $\bar{Q}$ is held constant, the trapped region shrinks, and in this case disappears as the viscosity ratio decreases to small values. We should keep in mind that not only is the size of the trapped region decreasing, but so is the pressure head against which the pump can pump.

3.7. *The reflux and trapping limits*

For a peristaltic pump with specified wave shape and wave speed there is a range of $\bar{Q}$ (or equivalently ΔP) where trapping occurs, and a range where reflux occurs, for a prescribed peripheral-layer thickness and viscosity ratio. Here we follow Shapiro *et al.* (1969) and determine the limits of the trapping and reflux regions in the space defined by $\bar{Q}/\bar{Q}_0$ and ϕ for the two-fluid pump.

Trapping limit

The trapping limit is given by the value of $\bar{Q}$ where $\psi = 0$ at some η just greater than zero. The shape of the trapped region is obtained by setting $\psi = 0$ with $\eta \neq 0$ in (2.8*a*):

$$\eta^2 = \frac{(\mu-1)\,H_1^2[3(q+H)-2H_1]+H^2[3(q+H)-2H]}{\mu(q+H)}. \tag{3.7}$$

For trapping to occur η^2 must be greater than zero at some ζ. Requiring that both the numerator and denominator in (3.7) be of the same sign so that η is real, and observing that the denominator goes through a maximum and minimum at $\zeta = \frac{1}{4}$ and $\frac{3}{4}$ respectively, leads to two conditions on $\bar{Q}$ for the existence of trapped fluid:

$$\bar{Q}^- < \bar{Q} < \bar{Q}^+, \tag{3.8a}$$

where

$$\bar{Q}^- = \frac{H_{1\,\max}^2(\mu-1)\,(2H_{1\,\max}-3\phi)+(1+\phi)^2\,(2-\phi)}{3(\mu-1)\,H_{1\,\max}^2+3(1+\phi)^2}, \tag{3.8b}$$

$$\bar{Q}^+ = \frac{H_{1\,\min}^2(\mu-1)\,(2H_{1\,\min}+3\phi)+(1-\phi)^2\,(2+\phi)}{3(\mu-1)\,H_{1\,\min}^2+3(1-\phi)^2}. \tag{3.8c}$$

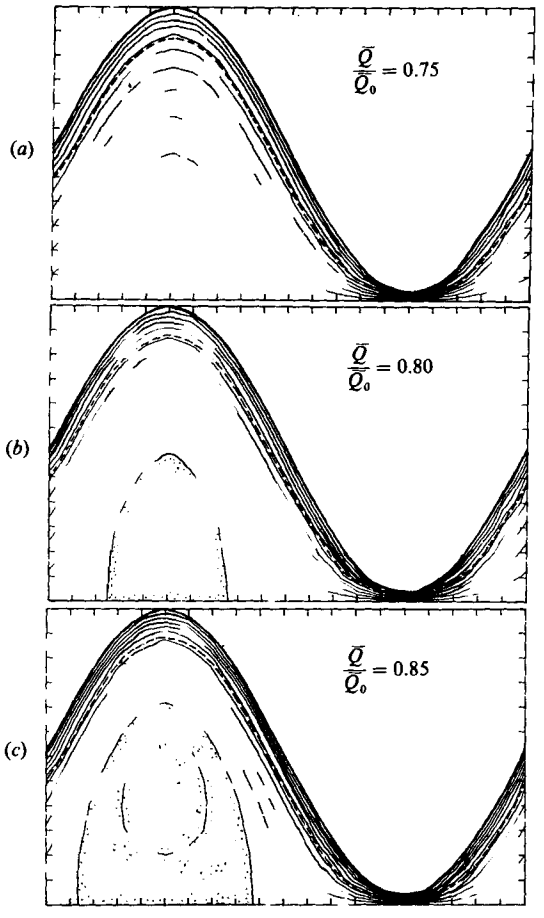

FIGURE 13. Streamlines in the wave frame showing the appearance of trapping (shaded region) at large-volume flow rates with a peripheral layer of low viscosity. $\bar{Q}_0$ = the maximum (positive) volume flow rate, obtained with $\Delta P = 0$ [equation (3.2*b*)]. $\phi = 0.95$, $\alpha = 0.8$, $\mu = 0.1$; ---, interface.

$H_{1\,\max}$ and $H_{1\,\min}$ refer to the values of H_1 at $\zeta = \frac{1}{4}$ and $\frac{3}{4}$ respectively. When $\mu = 1$, (3.8) reduces to the result given by Shapiro *et al.* (1969) for the single-fluid pump.

$\bar{Q}^-$ defines the trapping limit, the value of $\bar{Q}$ above which trapping occurs. Equation (3.8*b*) must be solved iteratively since $\bar{Q}^-$ is a function of H_1 which itself is a function of $\bar{Q}$. Having found the trapping limit Q^-, $\bar{Q}_0$ is obtained from (3.2*a*). The trapping limits at different viscosity ratios are given in figure 15. The area where trapping may be found is extended when μ increases and reduced when μ decreases. It is interesting that although the trapping area does not become very narrow in the limit $\mu \to 0$, it is still possible to have trapping when both $\bar{Q}/\bar{Q}_0$ and ϕ are large. In figure 14 conditions are such that the trapped region disappears as the viscosity ratio decreases.

Reflux limit

We found in §3.5 that reflux, when it exists, occurs in a layer adjacent to the wall and spreads inward as viscosity ratio increases. Thus, to find the reflux limit we expand $\bar{Q}_\psi$ about the wall in terms of the small parameter ϵ, where

$$\epsilon = \psi - q,$$

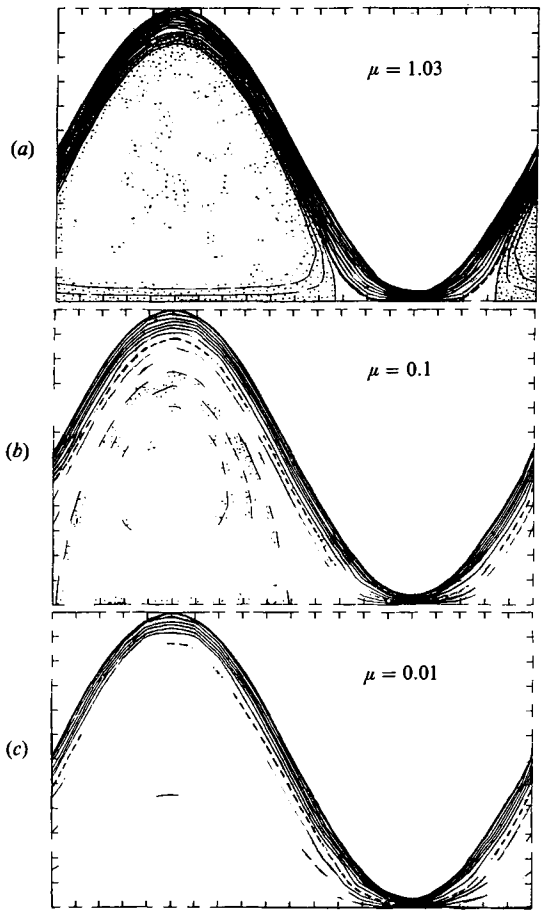

FIGURE 14. Streamlines in the wave frame showing the effect of viscosity ratio on trapping (shaded region), with fixed $\bar{Q}$. $\bar{Q}/\bar{Q}_0 = 0.9$, $\phi = 0.95$, $\alpha = 0.8$; , interface.

and apply the reflux condition

$$\frac{\bar{Q}_{\psi}}{\bar{Q}} > 1 \quad \text{as } \epsilon \to 0. \tag{3.9}$$

Using (2.8*b*), the first two terms in the expansion for $\eta(\zeta; \psi)$ are determined and the integration in (3.6) carried out to second order. (3.9) then yields the condition necessary for the occurrence of reflux:

$$\int_0^1 \frac{(\bar{Q}+H-1)\,H}{H^3+(\mu-1)\,H_1^3}\,\mathrm{d}\zeta < 0 \quad (\bar{Q} > 0). \tag{3.10}$$

The reflux limit is found iteratively by searching for the value of $Q \equiv \bar{Q}_R$ which makes (3.10) an equality. Once found, $\bar{Q}_0$ is obtained from (3.2*a*). In the limit $\mu \to 1$, (3.10) reduces to $\bar{Q} < \phi^2$ as derived by Shapiro *et al.* (1969).

The reflux limit becomes numerically unstable when ϕ is small since in the limit $\phi \to 0$ both $\bar{Q}_R$ and $\bar{Q}_0$ approach zero. Their ratio, however, is finite in this limit, and to find it requires a perturbation analysis around $\phi = 0$. The condition for reflux at $\phi = 0$ is found (see the Appendix) to be

$$\frac{\bar{Q}}{\bar{Q}_0} < 1-\frac{2}{3}\left\{\frac{[1+(\mu-1)\,\alpha^3]^2}{2+\alpha^3(\mu-1)\,[5+\alpha^2(2\mu-3)]}\right\}. \tag{3.11}$$

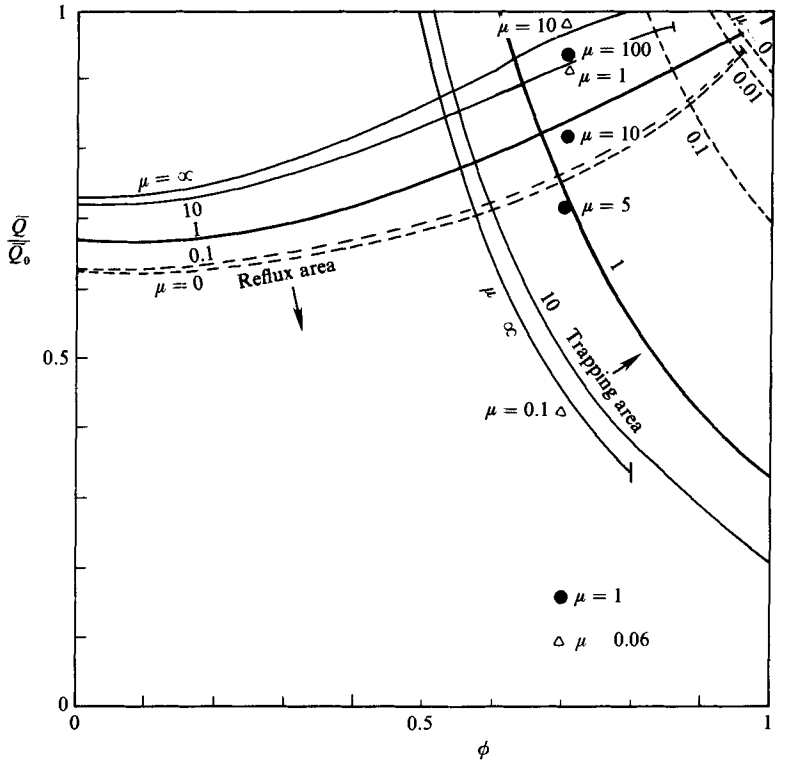

FIGURE 15. The parametric pumping range defined by $\bar{Q}/\bar{Q}_0$ and ϕ showing the areas in which reflux and trapping can occur with different viscosity ratios. The circles and triangles at $\phi = 0.7$ show the location of the pump with fixed ΔP when μ is varied. $\alpha = 0.8$; ●, $\Delta P = 10$; △, $\Delta P = 1$.

The reflux limit at different viscosity ratios is shown in figure 15. In the parameter space defined by $\bar{Q}/\bar{Q}_0$ and ϕ, an increase in viscosity ratio enlarges the area in which reflux may be found, while a decrease in viscosity decreases the reflux area. This is consistent with figure 12, where it was found that an increase in μ resulted in an overall increase in reflux, or the tendency for reflux to appear if not previously existing. In the single-fluid axisymmetric case reflux occurs for the entire domain $0 \leqslant \bar{Q}/\bar{Q}_0 \leqslant 1$, $0 \leqslant \phi \leqslant 1$ (Shapiro *et al.* 1969).

3.8. *Comparisons at constant pressure head*

The basic conclusion one may draw from figure 15 is that overall both reflux and trapping increase when viscosity ratio increases, and decrease when viscosity ratio decreases. This follows when comparisons are made at the same volume flow rate, which is equivalent to remaining fixed at a point in figure 15 while varying μ, and therefore ΔP.

Consider now comparisons among pumps at the same pressure head ΔP, so that an increase or decrease in μ is accompanied by an increase or decrease in $\bar{Q}$ respectively. To see qualitatively the effect of the peripheral layer on reflux and trapping, we have plotted a series of points at $\phi = 0.7$ in figure 15 which correspond to different values of μ when ΔP is held constant. The circles are for a constant ΔP of 10 and the triangles for a constant ΔP of 1. As μ increases, $\bar{Q}/\bar{Q}_0$ increases; the smaller the value of ΔP, the more rapid the increase.

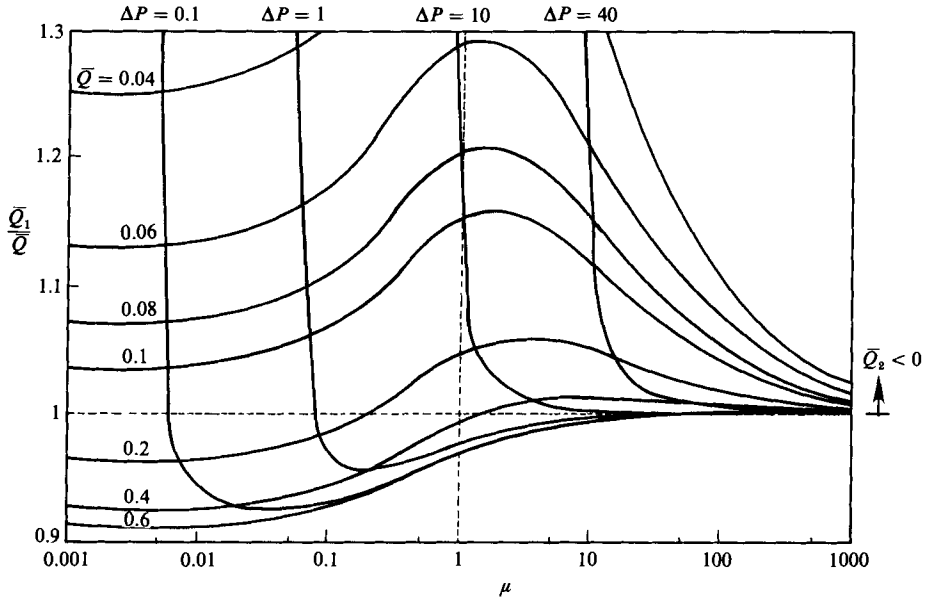

FIGURE 16. The variation with viscosity ratio of the average volume flow rate of the core fluid $\bar{Q}_1$ relative to the total volume flow rate $\bar{Q}$, with ΔP or $\bar{Q}$ held constant. Net reflux in the peripheral layer exists when $\bar{Q}_1/\bar{Q} > 1$. $\phi = 0.7$; $\alpha = 0.8$.

Qualitatively, the effect of the peripheral layer on trapping is the same with ΔP or $\bar{Q}$ held constant. As viscosity ratio increases, trapping increases, and as viscosity ratio decreases, trapping decreases. However, with fixed ΔP the movement into or out of the trapping area is much more rapid than at fixed $\bar{Q}$; and unlike the case $\bar{Q}$ = constant, a decrease in μ with constant ΔP always leads to the disappearance of trapping.

With regard to reflux, the effect of the peripheral layer with fixed pressure head is quite different from that at constant flow rate. Whereas a decrease in μ with fixed $\bar{Q}$ leads to a decrease or disappearance of reflux, at constant ΔP the peristaltic pump moves deep into the reflux region. Conversely, as μ increases with fixed ΔP, reflux weakens, and depending on the value of ΔP, may disappear.

This opposite effect of the peripheral layer on reflux, depending on whether ΔP or $\bar{Q}$ is held constant, is shown clearly in figure 16, where the ratio of the average volume flow rate of the core fluid to the total flow rate is plotted against μ with both ΔP and $\bar{Q}$ fixed. Since $\bar{Q} = \bar{Q}_1 + \bar{Q}_2$, net reflux in the peripheral layer occurs when $\bar{Q}_1/\bar{Q} > 1$. At constant $\bar{Q}$ reflux tends to appear at large μ when it did not previously exist at small μ, and reflux in general increases with increasing μ. This behaviour is analogous to figure 12, except that since $\bar{Q}_2 \to 0$ as $\mu \to \infty$, $\bar{Q}_1/\bar{Q} \to 1$.

The curves at constant ΔP, however, display quite a different behaviour. When reflux is already present in the peripheral layer, decreasing the viscosity ratio increases the relative amount of reflux. Even at low values of ΔP, when reflux is not present at large μ, reflux at some point appears and rapidly increases with decreasing μ. At the same time $\bar{Q}$ is decreasing towards zero. At the point where $\bar{Q}$ becomes negative, $\bar{Q}_1/\bar{Q} \to \infty$, so most of the reverse flow occurs in the peripheral layer.

This behaviour is clearly displayed in figure 17 where $\bar{Q}_1$, $\bar{Q}_2$ and $\bar{Q}$ are plotted against μ for ΔP fixed. When $\Delta P = 1$, $\bar{Q}_2 > 0$ so $\bar{Q}_1 < \bar{Q}$. However, when μ becomes

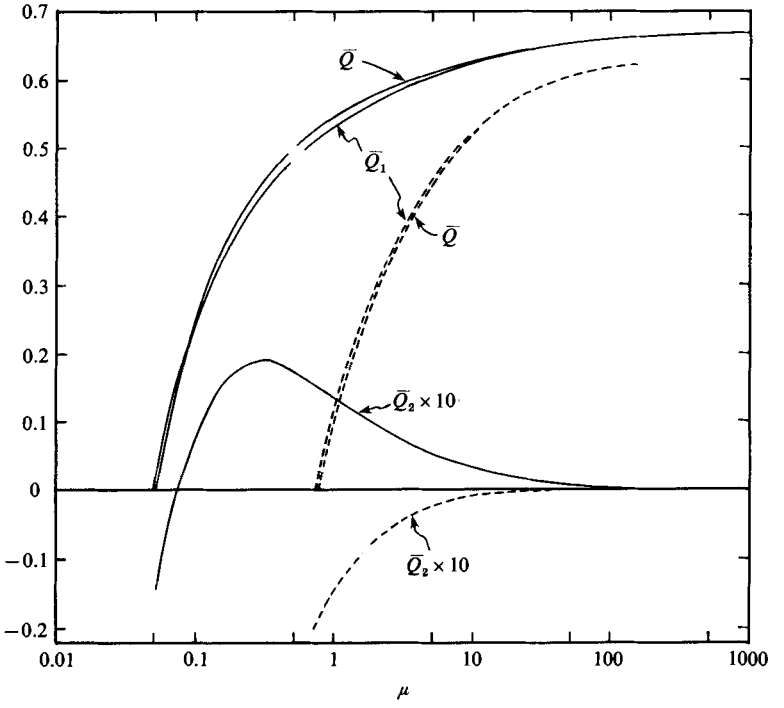

FIGURE 17. $\bar{Q}$, $\bar{Q}_1$ and $\bar{Q}_2$ plotted against μ for $\Delta P = 1$ ( ) and 10 ( ), where $\bar{Q}_1$ is the average volume flow rate in the core region, and Q_2 in the peripheral layer ($\bar{Q} = \bar{Q}_1 + \bar{Q}_2$). $\bar{Q}_2$ has been multiplied by 10 for clarity. $\phi = 0.7$; $\alpha = 0.8$.

sufficiently small, reflux appears, $\bar{Q}_2$ becomes negative and $\bar{Q}_1 > \bar{Q}$. When $\Delta P = 10$, net reflux exists in the peripheral layer at all μ so $\bar{Q}_1 > \bar{Q}$ everywhere.

Observe in figure 17 that the effect of the peripheral layer on the core fluid ($\bar{Q}_1$) is qualitatively the same as with both fluids combined ($\bar{Q}$). Again performance is improved by a more-viscous peripheral layer and degraded by a less-viscous peripheral layer.

4. Summary and conclusions

We have analysed the effect of a peripheral layer on peristaltic pumping of two Newtonian fluids at low Reynolds number and small curvature. The solution for the interface, which is dynamically consistent with the equations of motion and satisfies continuity, is described by a fourth-order algebraic equation, solvable by radicals. We consider only the case where the interface defines a peripheral layer that remains outside any region of trapped fluid that may exist. From the solutions for the velocity and pressure fields we draw conclusions for the pump operating in the range $0 < \bar{Q} < \bar{Q}_0$ and $0 < \Delta P < \Delta P_0$, where Q_0 and ΔP_0 are the maximum positive values when ΔP and $\bar{Q}$ are zero respectively.

In assessing the effect of the peripheral layer we must specify which conditions are to be held constant while comparing pumps. We hold the wave shape and wave speed constant while making comparisons first with fixed flow rate $\bar{Q}$, and then with fixed pressure head ΔP. The effect of the peripheral layer is not the same in the two comparisons.

4.1. *Pumping characteristics*

The pumping characteristics are summarized in figures 6 and 9. In general, the relationship between ΔP and $\overline{Q}$ is nonlinear and strongly dependent on viscosity ratio. As the viscosity ratio increases, pumping performance improves, which is to say that at fixed pressure head fluid is pumped at a higher volume flow rate, while at fixed volume flow rate the pump works against a greater pressure head, and the mechanical efficiency of the pump increases. As the viscosity ratio decreases, on the other hand, performance is badly degraded. In fact as $\mu \to 0$ the pressure head against which the pump can do work and the efficiency decrease to zero. Thus, if the pressure head is held constant and the viscosity ratio reduced, a point is reached where the pump no longer functions. Even a very thin peripheral layer can badly degrade pumping performance if the viscosity in the peripheral layer is small relative to the fluid being pumped (figure 10). The same conclusions follow when considering the effect of the peripheral layer on the core fluid alone (figure 17).

4.2. *Trapping*

We have found that in comparing pumps, either with the same $\overline{Q}$ or the same ΔP, the general trend is towards a reduction in trapping as the viscosity ratio decreases, and an increase in trapping as the viscosity ratio increases. The results are best summarized in figure 15, which shows that as μ decreases to zero the parameter domain in which trapping may be found shrinks to a small area at high values of $\overline{Q}$ and ϕ. Thus, except at these large values of ϕ and $\overline{Q}$, trapping will eventually disappear when the viscosity ratio becomes sufficiently small. The same trend occurs with fixed ΔP; however, trapping now always disappears for μ sufficiently small.

4.3. *Reflux*

As with the single-fluid pump, when reflux occurs it always appears adjacent to the wall. Holding $\overline{Q}$ fixed, this layer spreads inwards and the amount of reflux increases as the viscosity ratio increases. If not already in existence, reflux may appear, and then increase with increasing μ. These trends are summarized in figure 15, where the pumping area over which reflux can be found broadens as the viscosity ratio increases. When comparisons are made at fixed ΔP, however, the opposite trends are observed. An increase in viscosity ratio decreases the amount of reflux, and conversely for decreasing μ. Indeed, reflux always appears at sufficiently small viscosity ratios, then increases to large fractions of the total volume flow rate as the viscosity ratio decreases further. At the point where μ is so small that the total volume flow rate becomes negative, the reverse flow occurs primarily in the peripheral layer.

This work was supported by the Fluid Mechanics Program of National Science Foundation.

A final comment: J.G.B. would like to express his great pleasure in having worked with Stan Corrsin these last few years. He will be missed.

Appendix. The reflux limit at $\phi = 0$

To find the reflux limit from (3.10) in the limit $\phi \to 0$, we expand the reflux condition

$$I \equiv \int_0^1 \frac{(\overline{Q}+H-1)H}{H^3+(\mu-1)H_1^3}\,\mathrm{d}\zeta < 0 \tag{A 1}$$

in a perturbation series in ϕ, where $H = 1+\phi\sin 2\pi\zeta$, and

$$H_1 = \alpha + a_1\phi + a_2\phi^2 + \ldots. \tag{A 2}$$

The coefficients a_1 and a_2 are found through a perturbation analysis of (2.11) for small ϕ. Substituting the expansion for H_1 into (2.11) and equating coefficients at each order yields a zeroth-order equation equivalent to (2.12), and at higher orders

$$a_1 = A_1\sin 2\pi\zeta, \quad a_2 = A_2\sin^2 2\pi\zeta, \tag{A 3}$$

where A_1 and A_2 are complicated functions of μ, α, q_1 and $\overline{Q}$. Thus, when (A 2) is substituted into (A 1) and I expanded in ϕ, the terms involving $\int_0^1 a_1\,\mathrm{d}\zeta$ drop out, leaving

$$\frac{I}{\beta} = Q[1+f(\alpha,\mu,A_1,A_2)\,\phi^2] - \tfrac{1}{2}\{3\beta[1+(\mu-1)\,\alpha^2A_1]-1\}\,\phi^2+\ldots, \tag{A 4}$$

where $\beta = [1+\alpha^3(\mu-1)]^{-1} > 0$.

Replacing I in (A 1) with (A 4) and solving for $\overline{Q}$ leads to the reflux condition to second order

$$\overline{Q} < \tfrac{1}{2}\{3\beta[1+(\mu-1)\,\alpha^2A_1]-1\}\,\phi^2+\ldots. \tag{A 5}$$

A_1 to first order is

$$A_1 = \tfrac{1}{2}\alpha\beta[3+\alpha^2(2\mu-3)]. \tag{A 6}$$

In the single-fluid limit $\mu \to 1$ (A 5) reduces to the result $\overline{Q} < \phi^2$ of Shapiro *et al.* (1969).

To evaluate the reflux limit ratio $\overline{Q}_R/\overline{Q}_0$ we perform a similar perturbation analysis on $\overline{Q}_0$. Substituting (A 2) into (3.2*a*) and expanding the integrals in ϕ leads to the second-order result

$$\overline{Q}_0 = \tfrac{3}{2}\beta[1+(\mu-1)\,\alpha^2A_1]\,\phi^2+\ldots. \tag{A 7}$$

Both $\overline{Q}_R$ (found by making (A 5) an equality) and $\overline{Q}_0$ approach zero at the rate ϕ^2 as $\phi \to 0$. Thus, the ratio approaches a finite limit, given by (3.11).

REFERENCES

Birkhoff, G. & MacLane, S. 1963 *A Survey of Modern Algebra.* MacMillan.

Buthaud, H. 1971 The influences of unsymmetry, wall slope, and wall motion on peristaltic pumping at small Reynolds number. M.S. thesis, Department of Mechanics, The Johns Hopkins University.

Jaffrin, M. Y. 1973 Inertia and streamline curvature on peristaltic pumping. *Intl J. Engng Sci.* **11**, 681–699.

Jaffrin, M. Y. & Shapiro, A. H. 1971 Peristaltic pumping. *Ann. Rev. Fluid Mech.* **3**, 13–36.

Lykoudis, P. S. & Roos, R. 1970 The fluid mechanics of the ureter from a lubrication point of view. *J. Fluid Mech.* **43**, 661–674.

Shapiro, A. H., Jaffrin, M. Y. & Weinberg, S. L. 1969 Peristaltic pumping with long wavelengths at low Reynolds number. *J. Fluid Mech.* **37**, 799–825.

SHUKLA, J. B. & GUPTA, S. P. 1982 Peristaltic transport of a power-law fluid with variable consistency. *Trans. ASME* K: *J. Biomech. Engng* **104**, 182–186.

SHUKLA, J. B., PARIHAR, R. S., RAO, B. R. P. & GUPTA, S. P. 1980 Effects of peripheral-layer viscosity on peristaltic transport of a bio-fluid. *J. Fluid Mech.* **97**, 225–237.

TAYLOR, G. I. 1951 Analysis of the swimming of microscopic organisms. *Proc. R. Soc. Lond.* A **209**, 447–461.